Studies of Radicals Generated in Supersonic Flash Pyrolysis by Laser Induced Fluorescence Spectroscopy

Hee-Kyung Kim, Han-Cheol Kwon, Jong-Ho Park, Young-Sang Choi, and Jong-Ho Choi*

Department of Chemistry and Center for Electro- & Photo-Responsive Molecules, Korea University, 1, Anam-dong, Seoul 136-701, Korea

Received September 4, 1999

Laser-induced fluorescence (LIF) spectroscopy has been applied to study the supersonic jet of radicals of nitric oxide (NO) and atomic iodine produced in the flash pyrolysis of precursors n-butylnitrite ($CH_3(CH_2)_3ONO$) and allyl iodide (C_3H_5I), respectively. The systematic population analysis with spectral simulations demonstrates that the precursors are efficiently pyrolyzed and that radical beams show a substantial supersonic cooling. In addition, absence of local equilibrium was observed in the distributions of two electronic spin-orbit states $^2\Pi_{1/2}$ and $^2\Pi_{3/2}$ of NO products and can be rationalized in terms of the efficiency of collision-induced energy transfer rates.

Introduction

Reaction dynamics provides important insights into chemical reaction mechanism at the molecular level.[1] Especially studies on the reactive scattering between an atom and hydrocarbon radicals play a significant role in understanding organic synthesis, combustion, atmospheric and interstellar chemistry. Little information on reaction dynamics of radicals has, however, been known compared to the studies between an atom and stable closed-shell molecules.[2] The prerequisites for such studies are a clean and efficient generation of reactant radicals, and reliable and facile characterization schemes. Conventional pyrolytic effusion source experiences a long residence time inside a hot tube and is, therefore, inevitably susceptible to radical-radical recombination and/or secondary dissociation. In addition, since many hydrocarbon radicals have generally been known to undergo fast nonradiative relaxation processes after electronic excitation, sensitive photoluminescence detection methods can not be directly applied.

One useful scheme to overcome the problems due to the long residence is to utilize the supersonic flash pyrolysis technique developed by Chen in short-pulse experiments.[3] In the flash pyrolysis process, labile organic precursors entrained in a molecular beam spend a short residence time (~10 μsec) inside a hot cylindrical SiC tube and are efficiently decomposed to generate expansions of jet-cooled hydrocarbon radicals. Chen and coworkers obtained partially resolved electronic spectra for several hydrocarbon radicals by multiphoton ionization spectroscopy and found that in most cases the precursor is completely decomposed into radical products.[4] Barney Ellison *et al.* applied a FT-IR spectroscopy to study the pyrolysis of alkyl nitrite (RONO) and obtained the absorption spectra and the number density of radicals.[5] However, the information obtained is still limited and the characterization on the internal states of the radicals which is important in the studies of state-selective reaction dynamics is not absolutely clear.

In this paper, we describe our LIF spectroscopic investigations of the hydrocarbon radicals produced in supersonic flash pyrolysis. As our first example, we have studied the nitric oxide (NO) radicals seeded in helium. Since the LIF spectroscopy of NO has been well established,[6-8] it serves as a good test species to characterize our recently built molecular beam and pyrolysis sources. Next, we have generated organic radicals: n-butoxy ($CH_3(CH_2)_3O$) and allyl (C_3H_5). Those radicals are known to be reactive intermediates in many important chemical reactions. In particular, allyl has long attracted much photochemical and theoretical attention.[9-11] Allyl is the smallest π-conjugated system stabilized by two equivalent resonance structures and cyclization to cyclopropyl gives the simplest example of electrocyclization.

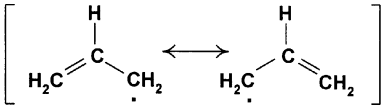

Since our target organic radicals do not exhibit fluorescence due to the fast non-radiative kinetic processes (for example, for allyl on the sub-100 psec scale),[12] instead, we have utilized precursor molecules with a weakly bound and LIF detectable component. We have chosen n-butyl nitrite ($CH_3(CH_2)_3ONO$) and allyl iodide (C_3H_5I) for n-butoxy and allyl, respectively. The bond dissociation energies (BDE) of the precursors are 42.5 kcal mol^{-1} (O-NO bond of n-butyl nitrite) and 43.5 kcal mol^{-1} (C-I bond of allyl iodide), respectively.[13] After flash decomposition nitric oxide and atomic iodine are quantitatively generated in a supersonic beam:

$$\text{n-}CH_3(CH_2)_3ONO \rightarrow \text{n-}CH_3(CH_2)_3O + NO \qquad (1a)$$

$$C_3H_5I \rightarrow C_3H_5 + I \qquad (1b)$$

Pyrolysis fragments NO and I can be detected through LIF spectroscopy and, therefore, act as useful probes for understanding the process of radical production.

Experimental Section

Schematic diagrams of the crossed molecular beam apparatus and flash pyrolysis source employed in the experiment are shown in Figures 1 and 2. The apparatus designed for investigations of reactive scattering consists of two source chambers and a scattering chamber. The source chambers are connected to a central scattering chamber at right angles. The source and scattering chambers are pumped by two 6-inch and one 10-inch baffled diffusion pumps, respectively and the average base pressure in the scattering chamber is maintained below 2×10^{-6} Torr. The sample gas is seeded in ultra high purity helium (UHP He: 99.999%) at 2 and 5 atm stagnation pressures and expands through a pulsed nozzle (0.8-mm diameter. General Valve Co.) into the SiC tube nozzle (1.0-mm diameter, 25-mm long. Carborundum Co.). The SiC tube with a resistively heated length of 10- to 15-mm is attached to the faceplate of the pulsed valve by a water-cooled Al_2O_3 tube as shown in Figure 2. The precursors (n-butyl nitrite and allyl iodide) are pyrolyzed as the gas flows through the SiC channel and undergo the supersonic expansion into the center of the scattering chamber. The pressure

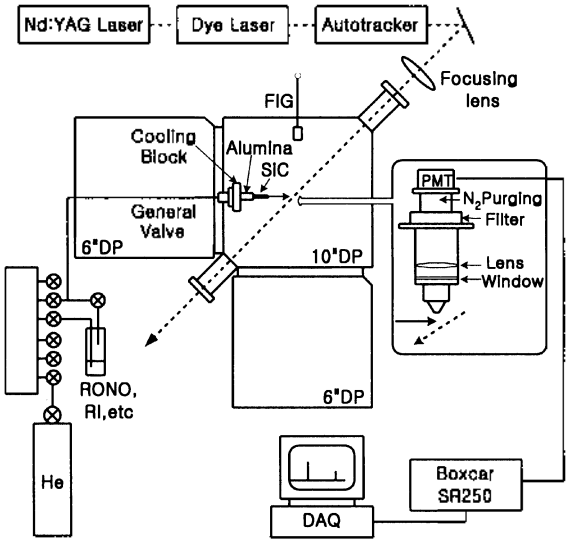

Figure 1. An overview of the crossed molecular beam apparatus.

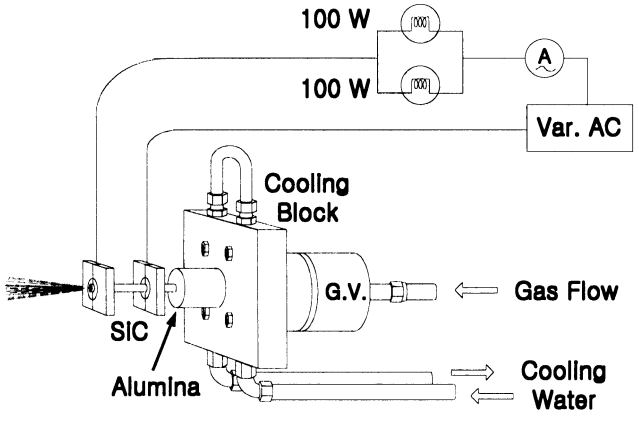

Figure 2. A schematic of the supersonic flash pyrolysis source.

in the central chamber is maintained at 3×10^{-5} Torr with the source operating at a repetition rate of 10 Hz. The pulse width of the supersonic jet is measured by the fast ion gauge based upon the design of Gentry.[14]

To characterize the molecular beam sources and the pyrolysis products from n-butyl nitrite (Aldrich), the LIF detection scheme *via* the $A^2\Sigma^+ \leftarrow X^2\Pi$ (0, 0) transition of NO was used. The output of the Nd:YAG laser pumped dye laser system (Continuum Surelite II-10, Spectron SL4000B) operating on coumarine 450 was frequency-doubled in a BBO crystal mounted on a home-made autotracker and slightly focused by a 50-cm lens into the center of the supersonic radical beam. To avoid the saturation in the fluorescence signal, the probe beam was carefully controlled and maintained below several tens μJ/pulse. The resulting fluorescence from the NO electronic transition was collected through a CaF_2 window and focused with a 20-cm focal length CaF_2 lens onto the PMT (Hamamatsu R166UH) placed in the direction perpendicular to the probe laser beam and the radical beam as shown in Figure 1. The signal from the PMT was sent to a boxcar averager (Stanford SR250) interfaced to an IBM-PC for display and analysis. Fluorescence spectra were obtained by scanning the dye laser wavelength and averaging the signal for 20 to 30 shots at each wavelength, depending on the signal intensity.

To detect the ground state atomic iodine ($^2P^0_{3/2}$) from the pyrolysis of allyl iodide (Aldrich), a two-photon absorption scheme was used.[15] The dye laser, operating on rhodamine 640, generated a beam that was frequency-doubled in a BBO crystal and focused with a 70-cm focal length CaF_2 lens into the center of atomic beam. While the electronic excitation was induced by a two-photon absorption at ~304 nm, the fluorescence from atomic iodine was monitored at ~178 nm. To prevent the VUV fluorescence attenuation by air while recording the LIF spectra, the telescope and PMT (Hamamatsu R166UH) housing were first evacuated and then continuously purged with nitrogen (N_2).[16]

Results and Discussion

Nitric Oxide (NO). A series of LIF scans for 3% NO at a stagnation pressure of 2 atm He have been taken at various nozzle-interaction region distances (30-90 mm) *without* a flash pyrolysis source. No significant change was observed in the fluorescence spectra, verifying that relaxation is minimal in our molecular beam. Figure 3 shows a typical LIF spectrum obtained at a nozzle-interaction distance of 30 mm, where the width of the beam pulse was measured to be about 850 μsec wide (full width at half maximum: fwhm). From the spectrum it is clear that only the low J'' (0.5 and 1.5) states in the ground electronic state ($X^2\Pi_{1/2}$: F_1) of NO are significantly populated, indicating that the rotational cooling of the NO/He beam is quite efficient. A more quantitative determination of the rotational state populations and the degree of cooling can be obtained from the analysis of the spectral lines. The relation between the observed line intensities and level populations depends on the extent of satura-

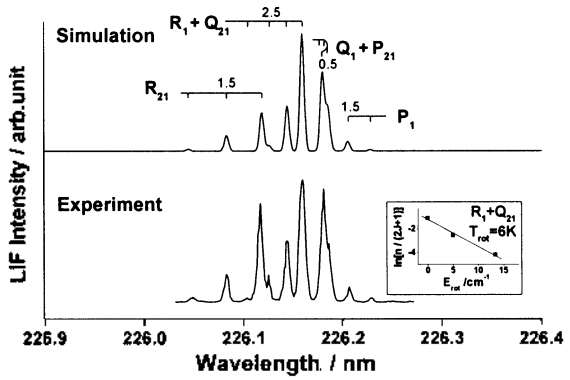

Figure 3. Experimental and simulated NO ($A^2\Sigma^+ \leftarrow X^2\Pi$ (0, 0)) spectra without a SiC tube.

tion.[7] The UV probe intensity used in our experiment was carefully controlled such that the excitation was unsaturated. Assuming constant laser intensity and neglecting polarization, quenching and weak frequency dependency, the rotational state population $n_{v''\Omega''}(J'')$ can be calculated from the following relation:

$$I_{LIF}\,(A^2\Sigma^+(v', J') \leftarrow X^2\Pi(v'', J'')) - C \cdot n_{v''\Omega''}(J'') \cdot q_{v'v''} \cdot S_{J'J''} \cdot (2J''+1)^{-1}$$

I_{LIF} is the observed LIF intensity in a $A^2\Sigma^+(v', J') \leftarrow X^2\Pi(v'', J'')$ transition of NO. The proportionality factor C includes all frequency independent experimental parameters. $q_{v'v''}$ is the Franck-Condon factor of the transition, which is constant within one band. $S_{J'J''}$ is the appropriate Hönl-London factor and $2J''+1$ is the rotational degeneracy of the lower electronic state. When a simple Boltzmann distribution is assumed, the rotational temperature can be determined through plotting $\ln|n_{v''\Omega''}(J'')/(2J''+1)|$ *vs* the rotational energy E_{rot} (cm^{-1}), with a slope corresponding to a rotational temperature of about 6 K as shown in Figure 3. At the NO rotational temperature, we also performed a spectral simulation of the $A^2\Sigma^+ \leftarrow X^2\Pi$ transition using known spectroscopic constants.[8] The simulation in Figure 3 closely matches the experimental spectrum and provides further confirmation in support of estimating the NO rotational temperature and the extent of the supersonic cooling (Table 1).

A systematic comparison of the rotational population analysis as a function of the heating power has been performed *with* a flash pyrolysis source for the same sample beams of 3% NO in He at a stagnation pressure of 2 atm. The LIF spectrum in Figure 4 displays the effect of the *unheated* SiC nozzle on the molecular beam. It was observed that slightly higher J'' states in $^2\Pi_{1/2}$ are populated compared to the spectrum in Figure 3 and that the pulse width measured at the same distance of 30 mm downstream shows a slightly broader distribution of about 950 μsec fwhm. The internal state populations can be well described by a straight line with a corresponding rotational temperature of around 10 K, which is also confirmed by the simulation shown in Figure 4. It is believed that the elongated beam in terms of pulse width (850 to 950 μsec wide) undergoes an adiabatic expansion with reduced collision frequency, resulting in a slightly

Table 1. Rotational temperatures of radicals at different heating powers and backing pressures

	Backing Pressure (atm)	SiC tube Heating (W)	Rotational Temperature (K)	
			$F_1(R_1+Q_{21})$	$F_2(Q_2+R_{12})$
3% NO/He	2	w/o SiC	6	0
		0	10	0
		9.5	100	140
		20	100	160
		32	120	175
	5	20	80	140
n-C_4H_9ONO	2	20	170	210
	5	20	85	170
		30	105	170
C_3H_5I*	2	20	150	

ref. 22)

hotter jet. However, the extent of the overall cooling is still very significant and the effectiveness is demonstrated by the absence of the spectral lines from the upper electronic state ($X\,^2\Pi_{3/2}$: F_2 at 121 cm^{-1}) of NO (Table 1).

As the SiC nozzle is heated, the sample gas mixture absorbs the heat energy from the hot cylindrical wall through thermalizing collisions. Under the typical experimental conditions, the SiC wall temperature was estimated to be as high as 1500 K.[5] Since the important temperature is the internal temperature of the sample molecules in the gas flow, the dynamics of the heat transfer from wall to sample is believed to determine the efficiency for the heat absorption and the processes of decomposition. Barney Ellison *et al.* performed approximate calculations for the 1% N_2O/He flow at the wall temperature of 1500 K and found out that the gas absorbs a significant amount (about 80%) of heat from the tube wall during a short passage time of 20 μsec and that the internal temperature reaches around 800 K.[5] Although 3% NO diluted in He is used in our experiment, the dilution will not significantly change the estimation, signifying that our beam is believed to be internally excited due to the heat transfer from the hot SiC tube.

A series of the experimental LIF spectra as a function of

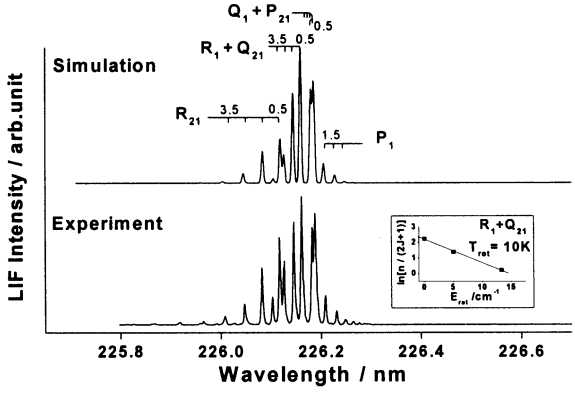

Figure 4. Experimental and simulated NO ($A^2\Sigma^+ \leftarrow X^2\Pi$ (0, 0)) spectra with an unheated SiC tube.

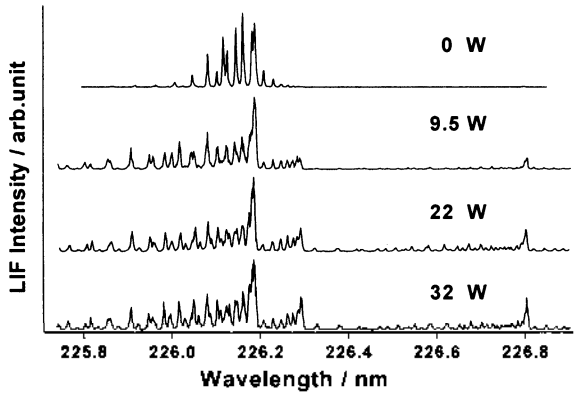

Figure 5. The dependence of the NO ($A^2\Sigma^- \leftarrow X^2\Pi$ (0, 0)) LIF spectra on the pyrolysis heating power.

the heating power (Fig. 5) exhibit such internal excitation of the jet: the observation of the spectral transitions from the electronically excited $^2\Pi_{3/2}$ state and the broad rotational population distribution in each spin-orbit state. In particular the P_1 bandhead of $^2\Pi_{1/2}$ and the $P_2 + Q_{12}$ bandhead of $^2\Pi_{3/2}$ in the spectra (assigned in Fig. 6) are sensitive measures of rotational excitations. The gradual increase in each bandhead height is observed as the heating power is increased. In determining the rotational temperatures, the population distribution in the excited $^2\Pi_{3/2}$ state was found to be different from that in the ground $^2\Pi_{1/2}$ state. Table 1 lists the obtained estimates of the rotational temperatures in each electronic state at three different heating powers and shows the higher rotational temperatures of the excited $^2\Pi_{3/2}$ state. One spectral simulation using two different rotational temperatures at the heating power of 20 W displays a good agreement with the experimental spectrum (Fig. 6). The observation of non-equilibrium between the two spin orbit $^2\Pi_{1/2}$ and $^2\Pi_{3/2}$ states can be explained by the different collision-induced energy transfer rates.[17] For NO/He expansion the energy transfer rate from one spin-orbit manifold to the other is known to be about ten times smaller than that within the same manifold. As the jet expansion proceeds, therefore, the lower J states of the $^2\Pi_{3/2}$ are quite inefficient in the energy transfer to the rotational states of the $^2\Pi_{1/2}$, leading to the lack of local equilibrium between the two spin-orbit states. The extent of the rotational cooling has also been examined by changing the expansion parameter ($P_s \cdot d$), where P_s is the nozzle stagnation pressure and d is the nozzle diameter. It is well known that the internal temperature of the supersonic molecular beam decreases with increasing the expansion parameter.[18] As can be seen in Table 1, the rotational temperatures in both spin-orbit states decrease by 20 K at the heating power of 20 W with increasing the stagnation pressure from 2 to 5 atm.

n-Butyl Nitrite ($CH_3(CH_2)_3ONO$). The pyrolysis of n-butyl nitrite is initiated by the breaking of the weakest bond of RO-NO (BDE = 42.5 kcal mol^{-1}), resulting in the generation of nitric oxide and butoxy radicals as indicated in Eq. (1a). To obtain the extent of the precursor fragmentation under our experimental conditions, we examined the unimolecular reaction kinetics of n-butyl nitrite. Batt and co-workers studied the decomposition kinetics of a series of alkyl nitrites in a static system and obtained the rate constant for n-butyl nitrite: $k_d(T) = 1 \times 10^{16} \cdot \exp[-41.8\ \text{kcal/mol}/(RT)]$.[19] If we assume that the internal temperature of n-butyl nitrite is heated up to 800 K during the passage (residence) time of 20 μsec, then the unimolecular reaction proceeds through the following equation

$$[P] = [P]_o \exp[-k_d(T)t]$$

and leads to the decomposition such that the initial nitrite precursor $[P]_o$ is completely pyrolyzed into NO and n-butoxy radicals. Here further reaction of n-butoxy radical is neglected.

Figure 7 displays the observed spectrum of the pyrolysis product NO at the heating power of 20 W. In the experiment no LIF signal was detected without heating, indicating that the NO spectrum shown in Figure 7 was the direct outcome of the precursor pyrolysis. The intensity of the signal and the spectral distribution increase as the heating power is increased. The rotational population distributions of the experimental spectra were analyzed in the same manner as described in the previous section and the results are shown in Table 1. The rotational temperatures in the two electronic $^2\Pi_{1/2}$ and $^2\Pi_{3/2}$ states are found to be different as in the case of 3% NO/He beam and decrease as the expansion parameter is increased. The lack of local equilibrium between the two spin-orbit states can be understood in terms of the different

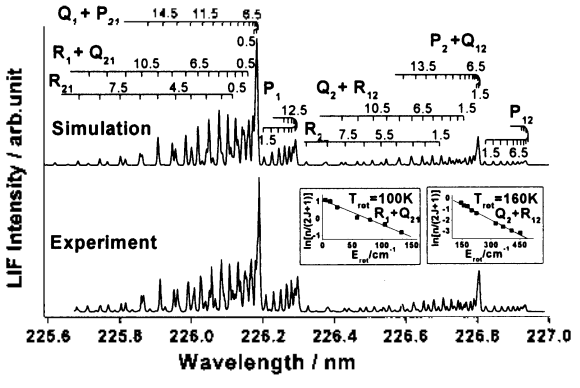

Figure 6. Experimental and simulated NO ($A^2\Sigma^- \leftarrow X^2\Pi$ (0, 0)) spectra at 20 W.

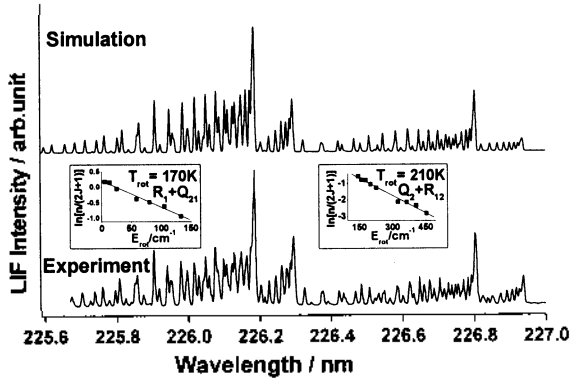

Figure 7. Experimental and simulated spectra of the fragment NO ($A^2\Sigma^+ \leftarrow X^2\Pi$ (0, 0)) from the flash pyrolysis of n-butyl nitrite at 20 W.

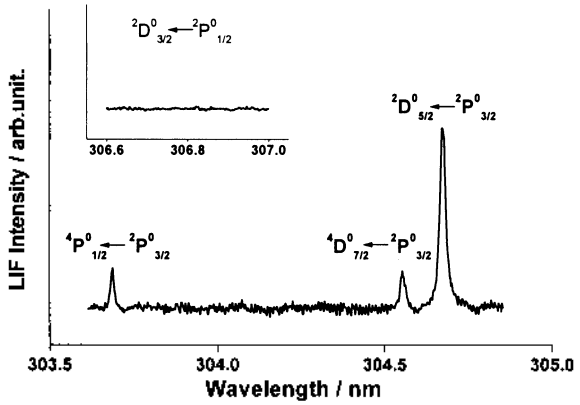

Figure 8. Two-photon LIF spectrum of atomic iodine generated in flash pyrolysis of allyl iodide.

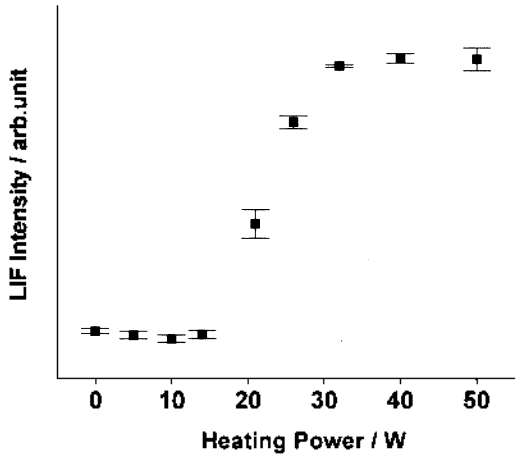

Figure 9. The dependence of the 304.7 nm peak intensity on the pyrolysis heating power.

collision-induced energy transfer rate as described in the previous section. A similar temperature in the $^2\Pi_{1/2}$ state was also observed in the pyrolysis experiments of ethyl nitrite using FT-IR spectroscopy performed by Barney Ellison and coworkers.[5] However, the distribution in the $^2\Pi_{3/2}$ state was found to be higher than 300 K, which was attributed to the inefficient cooling in their expansion chamber. To our knowledge our pyrolysis experiment is the first characterization of the incomplete equilibrium between the two spin-orbit states of radical products generated in the flash pyrolysis of precursor molecules.

Allyl Iodide (C_3H_5I). Pyrolysis of allyl iodide produces allyl and atomic iodine quantitatively and a typical two-photon LIF spectrum of ground-state atomic iodine ($^2P^0_{3/2}$) in the 303-307 nm region is displayed in Figure 8. The observed transitions are clearly resolved and assigned by comparison with published frequencies by Moore.[20] The large peak at 304.7 nm is originated from the $^2D^0_{5/2} \leftarrow {}^2P^0_{3/2}$ transition. Other higher frequency peaks are weaker due to the transitions between different spin multiplicities. The first excited spin-orbit state ($^2P^0_{1/2}$), by 7603.2 cm^{-1} from the ground state, was expected to lead to a transition of $^2D^0_{3/2} \leftarrow {}^2P^0_{1/2}$ at 306.7 nm, if populated. No peak was observed, since the heating in our pyrolysis experiments was not sufficiently high enough to overcome the energy difference. The absence is consistent with the recent results from pyrometry or time-of-flight (TOF) measurements,[9] where the upper limit of the internal temperature inside the pyrolysis tube was determined to reach 1000 to 1500 K ($E_{thermal}$ ~600-900 cm^{-1}).

Since atomic iodine does not have an internal structure, the dependency of the peak intensity on the heating power can be used to obtain the information about the extent of precursor decomposition. Figure 9 shows the dependency of the 304.7 nm peak intensity on the heating power. The substantial LIF signal began to appear at 20 W. After a sharp increase proportional to the heating power, we observed saturation in the 30-50 W region, indicating that the precursor was completely pyrolyzed at high power. The same behavior was observed in the TOF experiments,[9] where under the similar heating conditions the parent precursor ions ($C_3H_5I^+$) totally disappeared in the mass spectrum. The powers for allyl iodide are also consistent with those powers observed for n-butyl nitrite and hydrogen peroxide (HO-OH). Especially the O-O bond (BDE = 51 ± 1 kcal mol^{-1}) of H_2O_2 is stronger compared to the C-I bond of allyl and the pyrolysis behavior investigated through the OH LIF spectroscopy ($A^2\Sigma^+ \leftarrow X^2\Pi$) showed that the threshold and saturation powers are 40 W and 70 W, respectively, higher compared to those of n-butyl nitrite and allyl iodide with weaker bonds.[21] The rotational temperature of allyl can not be estimated in our experiment. However, a fit to the partially rotationally resolved ionization spectra obtained by Chen and coworkers results in a rotational temperature of 150 K quite comparable to the temperature observed in our pyrolysis of n-butyl nitrite (Table 1).[22]

In summary, we studied the supersonic jet of nitric oxide and atomic iodine produced in the pyrolysis of n-butyl nitrite and allyl iodide by applying LIF spectroscopy and demonstrated that organic radicals can be prepared efficiently from supersonic flash pyrolysis. We also obtained the optimized experimental conditions for the radical productions through the spectroscopic investigations. The strategy utilizing precursor molecules with weakly bound, LIF detectable components will be applied to synthesis of pure organic radicals and studies on reactive scattering of radicals in gas phase. Several organic radical systems and the reaction dynamics of allyl with ground electronic state oxygen atom ($O(^3P)$) produced by photodissociation of NO_2 are currently under investigation.

Acknowledgment. We would like to thank Dr. H. Reisler, Dr. C. J. Yoon, Dr. I. Fischer, Dr. S. K. Kim, Center for Electro- and Photo-Responsive Molecules (CRM) and Korea University for their invaluable help and discussion in the development of the crossed beam apparatus. The authors wish to acknowledge the financial support of the Korea Research Foundation in the program year of 1997.

References

1. Levine, R. D.; Bernstein, R. B. *Molecular Reaction Dynam-*

ics and Chemical Reactivity; Oxford University Press: New York, 1987.
2. Lee, Y. T. *Science* **1987**, *236*, 793.
3. Kohn, D. W.; Clauberg, H.; Chen, P. *Rev. Sci. Instrum.* **1992**, *68*, 4003.
4. (a) Chen, P.; Colson, S. D.; Chupka, W. A.; Berson, J. A. *J. Phys. Chem.* **1986**, *90*, 2319. (b) Minsek, D. W.; Chen, P. *J. Phys. Chem.* **1993**, *97*, 13375.
5. Rohrs, H. W.; Wickham-Jones, C. T.; Ellison, G. B.; Berry, D.; Argrow, B. M. *Rev. Sci. Instrum.* **1995**, *66*, 2430.
6. (a) Irvine, A. M. L.; Smith, I. W. M.; Tuckett, R. P. *J. Chem. Phys.* **1990**, *93*, 3187. (b) Chou, M. S.; Dean, A. M.; Stern, D. *J. Chem. Phys.* **1983**, *78*, 5962.
7. Hunter, M.; Reid, S. A.; Reisler, H. *J. Chem. Phys.* **1993**, *99*, 1093.
8. Suchard, S. N. In *Spectroscopic data (vol. 1)*; IFI/Plenum: New York, 1975.
9. Stranges, D.; Stemmler, M.; Yang, X.; Chesko, J. D.; Suits, A. G.; Lee, Y. T. *J. Chem. Phys.* **1998**, *109*, 5372, and references therein.
10. (a) Deyerl, H. J.; Fischer, I.; Chen, P. *J. Chem. Phys.* **1999**, *110*, 1450. (b) Schultz, T.; Fischer, I. *J. Chem. Phys.* **1997**, *107*, 8197. (c) Deyerl, H. J.; Gilbert, T.; Fischer, I.; Chen, P. *J. Chem. Phys.* **1997**, *107*, 3329.
11. (a) Yamaguchi, M. *J. Mol. Struct. (Theochem.)* **1996**, *365*, 143. (b) Longuet-Higgins, H. C.; Abrahamon, E. W. *J. Am. Chem. Soc.* **1965**, *87*, 2045.
12. Schultz, T.; Fischer, I. *J. Chem. Phys.* **1998**, *109*, 5812.
13. Benson, S. W. In *Thermochemical Kinetics*; Wiley-International: 1976.
14. Gentry, W. R.; Giese, C. F. *Rev. Sci. Instrum.* **1978**, *49*, 595.
15. Brewer, P.; Das, P.; Ondrey, G.; Bersohn, R. *J. Chem. Phys.* **1983**, *79*, 720.
16. Okabe, H. *Photochemistry of Small Molecules*; Wiley-International publication: New York, 1978.
17. Zacharias, H.; Loy, M. M. T.; Roland, P. A.; Sudbo, A. S. *J. Chem. Phys.* **1984**, *81*, 3148.
18. (a) Baer, T.; Hase, W. L. *Unimolecular Reaction Dynamics*; Oxford University Press: New York, 1996. (b) Levy, D. H. *Ann. Rev. Phys. Chem.* **1980**, *31*, 197. (c) Engelking, P. C. *Chem. Rev.* **1991**, *91*, 399.
19. (a) Batt, L.; Milne, R. T.; McCulloch, R. D. *Int. J. Chem. Kinet.* **1977**, *9*, 567. (b) Batt, L.; Milne, R. T. *Int. J. Chem. Kinet.* **1977**, *9*, 549.
20. Moore, C. E. In *Atomic Energy Levels*; Natl. Bur. Stand. 35 (U.S. GPO. Washington, D.C., 1971) Vol. 3.
21. Kim, H. K.; Kwon, H. C.; Park, J. H.; Choi, J. H. (to be submitted).
22. Minsek, D. W.; Blush, J. A.; Chen, P. *J. Phys. Chem.* **1992**, *96*, 2025.